Synthetic antiferromagnetic nanoparticles with tunable susceptibilities

Wei Hu,[1,a)] Robert J. Wilson,[1] Christopher M. Earhart,[1] Ai Leen Koh,[1,2] Robert Sinclair,[1] and Shan X. Wang[1,3]
[1]*Department of Materials Science and Engineering, Stanford University, Stanford, California 94305, USA*
[2]*Department of Mechanical Engineering, Stanford University, Stanford, California 94305, USA*
[3]*Department of Electrical Engineering, Stanford University, Stanford, California, 94305, USA*

(Presented 13 November 2008; received 7 October 2008; accepted 19 November 2008; published online 6 February 2009)

High-moment monodisperse disk-shaped Co–Fe magnetic nanoparticles, stable in aqueous solution, were physically fabricated by using nanoimprinted templates and vacuum deposition techniques. These multilayer synthetic antiferromagnetic nanoparticles exhibit nearly zero magnetic remanence and coercivity, and susceptibilities which can be tuned by exploiting interlayer magnetic interactions. In addition, a low cost method of scaling up the production of sub-100 nm synthetic antiferromagnetic nanoparticles is demonstrated. © *2009 American Institute of Physics*.
[DOI: 10.1063/1.3072028]

I. INTRODUCTION

Magnetic nanoparticles have been actively investigated in biological and biomedical applications such as magnetic resonance imaging, biomagnetic separation and sensing, magnetic hyperthermia, and drug delivery.[1–5] These applications usually prefer monodisperse nanoparticles with high magnetic moments. Compared with widely used iron oxide nanoparticles, metallic magnetic nanoparticles (such as Co, Fe, and their alloys) possess much larger saturation magnetization and thus are promising for biomedical applications.[6–8] Metallic magnetic nanoparticles are commonly synthesized by chemical routes which are powerful, but the size of these nanoparticles is often limited to below 20 nm. Beyond this size, it is difficult to attain monodispersity and the onset of ferromagnetism results in coercivity, remnant magnetization and consequent magnetically induced agglomeration.

Magnetic susceptibility is an indicator of the sensitivity of magnetization to changes in an external magnetic field. Therefore, magnetic nanoparticles with tunable susceptibility are highly desirable in biological and biomedical applications. For superparamagnetic nanoparticles, tuning the susceptibility usually requires a change in size, shape, or composition, which is often limited by the synthesis methods or size distribution.

In this work we developed a direct physical fabrication of monodisperse disk-shaped synthetic antiferromagnetic (SAF) nanoparticles with high moment ferromagnetic constituents ($Co_{90}Fe_{10}$) and good stability in aqueous solutions. These nanoparticles are ~120 nm in diameter, which is well above the superparamagnetic size limit, but they are designed to exhibit zero magnetic remanence and coercivity. They also possess tunable magnetic susceptibilities, which creates the possibility of multiplex magnetic sorting.

[a)]Author to whom correspondence should be addressed. Electronic mail: weihu9@gmail.com.

II. EXPERIMENT

Synthetic Co–Fe nanoparticles were fabricated by using nanoimprint lithography and vacuum deposition followed by release and stabilization of nanoparticles in solution, as schematically illustrated in Fig. 1. A silicon substrate was first vacuum coated with a 50 nm chemically etchable release layer of copper and a thin surface layer of tantalum. Ta promotes the adhesion of resists and prevents oxidation and roughening of the Cu during resist bakes. Thermal nanoimprinting of a quartz stamp into a spin coated bilayer resist, a polymethyl methacrylate mask layer and a polymethylglutarimide underlayer, produces a template. The quartz stamp, with a patterned area of 1 cm^2 containing 10^9 pillars with 100 nm diameters and 200 nm heights, and the nanoimprinting tool were purchased from Obducat. Substrate bound magnetic nanoparticles were then fabricated by vacuum sputtering magnetic films, lift-off of continuous metal films, and removal of resists. The final step was to release the particles by ion milling through the thin Ta buffer layer and then

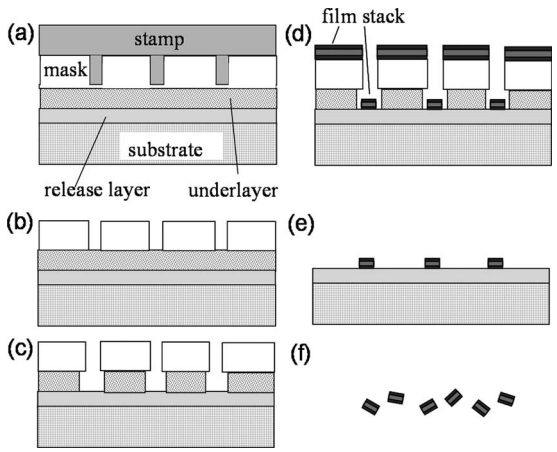

FIG. 1. Procedures for synthetic nanoparticle fabrication: (a) template formation by nanoimprint lithography, (b) residue layer removal by O_2 plasma, (c) undercut profile creation in the underlayer resist, (d) metal film deposition, and (e) lift-off followed by (f) chemically etching release layer.

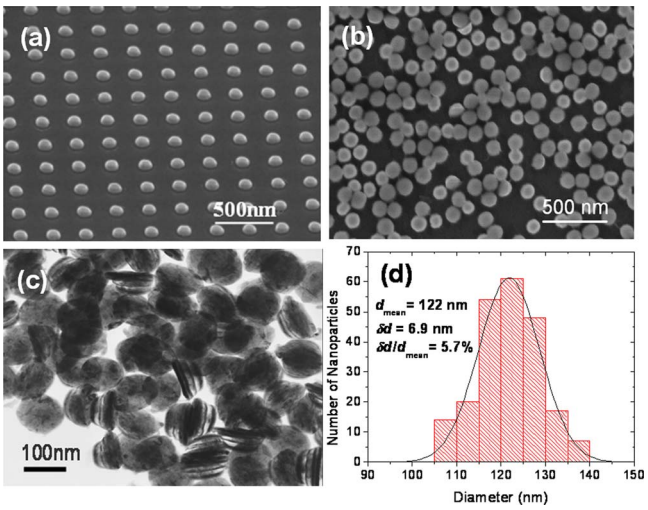

FIG. 2. (Color online) SEM images of 120 nm CoFe nanoparticles (a) bound to the substrate and (b) after release and collection in aqueous solution. (c) TEM image of released nanoparticles with the structure of Ta 5/Ru 2/Co–Fe 12/Ru 2.5/Co–Fe 12/Ru 2/Ta5 (thicknesses in nanometers) and (d) the corresponding size distribution.

chemically etching the Cu release layer with an ammonia-$CuSO_4$ solution. This etch was neutralized by the addition of citrate buffer, which also acts as a surfactant to stabilize the nanoparticles in solution. The particles were collected by multiple cycles of centrifugation, solvent exchange, and resuspension.

To obtain a clear view of the structure, shape, and size of these nanoparticles, scanning electron microscope (FEI XL30) and transmission electron microscope (Philips CM20) images were obtained. The magnetic properties were measured at room temperature with an alternating gradient magnetometer from Princeton Measurements.

III. RESULTS AND DISCUSSION

The basic structure of fabricated SAF nanoparticles includes two or multiple layers of ferromagnetic $Co_{90}Fe_{10}$ separated by a nonmagnetic spacer layer of Ru. Figure 2(a) shows an scanning electron microscopy (SEM) image of 120 nm defect-free nanoparticles bound to the substrate after metal lift-off. Figure 2(b) shows the corresponding nanoparticles after release into aqueous solution. A transmission electron microscopy (TEM) image in Fig. 2(c) shows an example of synthetic nanoparticles consisting of Ta 5/Ru 2/$Co_{90}Fe_{10}$ 12/Ru 2.5/$Co_{90}Fe_{10}$ 12/Ru 2/Ta 5 (thicknesses in nanometers). Ta is used for chemical and magnetic stabilities in solution. The multilayer structure is clearly preserved with negligible sidewall corrosion after the releasing process. The shape and size uniformities of these nanoparticles are largely determined by the quality of the stamps and deposition systems. Statistical measurements with SEM [Fig. 2(d)] show that synthetic nanoparticles have a very narrow diameter distribution of 5.7%, which is desirable for biomedical applications.

SAF nanoparticles exhibit zero magnetic remanence and adjustable magnetic properties over a wide range of sizes. These properties are controlled using interlayer magnetic interactions which depend on multilayer film structure and materials.[9] Figure 3(a) shows the typical magnetization curve of SAF nanoparticles with the structure of Ta 5/Ru 2/$Co_{90}Fe_{10}$ 12/Ru 2.5/$Co_{90}Fe_{10}$ 12/Ru 2/Ta 5 (thicknesses in nanometers). Without an applied field, these nanoparticles show nearly zero magnetic remanence and coercivity. As the external field is gradually increased, the moments of the individual ferromagnetic layers scissor toward the direction of the applied field until they are in a parallel configuration at the saturation field. This results in a nearly linear field dependence of the magnetization. The interactions between ferromagnetic layers under consideration include two forms: magnetostatic interactions through repulsion (attraction) of like (opposite) poles and interlayer exchange coupling mediated by a special nonmagnetic spacer layer. The strength of magnetostatic interactions depends roughly on the aspect ratio of the magnetic layer thickness (t) and the diameter (D) of the particle, whereas the interlayer exchange coupling strength critically depends on the spacer layer material and thickness, and the number of interfaces.

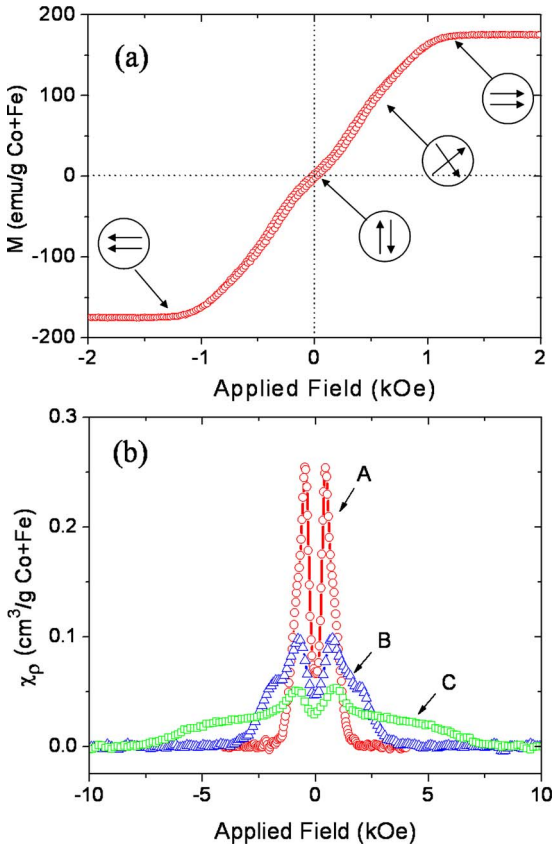

FIG. 3. (Color online) (a) *M-H* loops of 120 nm diameter SAF nanoparticles with the structure of Ta 5/Ru 2/$Co_{90}Fe_{10}$ 12/Ru 2.5/$Co_{90}Fe_{10}$ 12/Ru 2/Ta 5 (in nanometers). (b) Susceptibility (normalized by the mass of Co+Fe) vs in-plane applied field demonstrating tunability of the susceptibility through interlayer magnetic interactions. The structures of the samples are listed with total thickness in nanometers: curve A (circle): Ta 5/Ru 2/CoFe 6/Ru 2.5/CoFe 6/Ru 2/Ta 5, total of 28.5 nm; curve B (triangle): Ta 5/Ru 2/CoFe 6/Ru 0.6/CoFe 6/Ru 2/Ta 5, total of 26.6 nm; and curve C (square): Ta 5/Ru 2/[CoFe 3/Ru 0.6]3/CoFe 3/Ru 2/Ta 5, total of 27.8 nm.

Figure 3(b) shows plots of the field dependence of susceptibility ($\chi = dM/dH$, normalized by the mass of Co+Fe) of three different SAF nanoparticles. The susceptibilities of SAF nanoparticles often show a double peak characteristic,

which is distinctive from that of the superparamagnetic nanoparticles (single peak at zero field given by Langevin function). The valley of the susceptibility is due to a nonzero "spin flop" field associated with as deposited anisotropies,[10] which causes the magnetization curve to deviate from linearity at small fields, as shown in Fig. 3(a). By controlling the interlayer magnetic interactions the susceptibility of SAF nanoparticles can be tuned over a wide range, while maintaining constant saturation moments and nanoparticle sizes. For example, curve A in Fig. 3(b) represents SAF nanoparticles with 2.5 nm Ru where magnetostatic interactions between the two ferromagnetic layers dominate. The susceptibility curve [B in Fig. 3(b)] flattens by reducing the Ru spacer layer thickness to 0.6 Å where strong antiferromagnetic interlayer exchange coupling starts to take over. It can be further flattened and extended to higher fields by increasing the number of interfaces and magnetic layers [C in Fig. 3(b)]. These synthetic nanoparticles create the possibility of multiplex magnetic separation of biomolecules or cells where nanoparticles with different susceptibilities will possess distinct magnetophoretic velocities.[11] Because the diameter of SAF nanoparticles tends to be significantly greater than that of superparamagnetic nanoparticles, and the large saturation moments can be controlled independent of the susceptibility, the magnetophoretic velocities of SAF nanoparticles are also much larger than those of superparamagnetic nanoparticles with a typical diameter of <20 nm.

One outstanding practical issue relates to the prospects for obtaining large quantities of such particles with high efficiency and at reasonable cost. The 1 cm^2 quartz stamp used in this work, which was fabricated by electron beam lithography (at a cost of $10 000), can only provide a very limited number of particles ($\sim 10^9$) for each imprinting cycle. Cost for fabrication of larger stamps (e.g., 4 in. wafer) with dense nanopillars using e-beam lithography will be prohibitively high. Here we demonstrate a low cost method for producing large area silicon nanoimprint stamps containing nanopillar arrays by nanosphere lithography, as shown in Fig. 4. In this method, a nearly close-packed monolayer of sub-200 nm latex nanospheres formed on a silicon wafer by spin coating. The size of the nanospheres was reduced via reactive ion etching with a mixture of O_2 [50 SCCM (SCCM denotes cubic centimeter per minute at STP)] and CHF_3 (30 SCCM) gases. An array of sub-100 nm silicon pillars were finally fabricated by etching the underlying silicon with NF_3 (30 SCCM) gas using the reduced latex spheres as a mask. This method yields a 100 fold increase in the number particles per imprinting cycle. Combined with a polymer release layer to substitute Cu, which allow us to eliminate several of the deposition and etch steps already described, and a batch-process deposition scheme, we have successfully scaled up the production of SAF nanoparticles at high throughput and reasonable cost.[12]

IV. CONCLUSIONS

We developed a method for direct fabrication of high moment zero remanence monodisperse synthetic magnetic nanoparticles based on template patterning and high vacuum deposition of ferromagnetic materials followed by release and stabilization in aqueous solution. Interlayer magnetic interactions were explored to construct nanoparticles with sizes well above the superparamagnetic limit, while exhibiting zero remnant magnetization and widely tunable susceptibilities. SAF nanoparticles create the possibility of multiplex magnetic separation of biomolecules or cells if their surfaces are further functionalized.

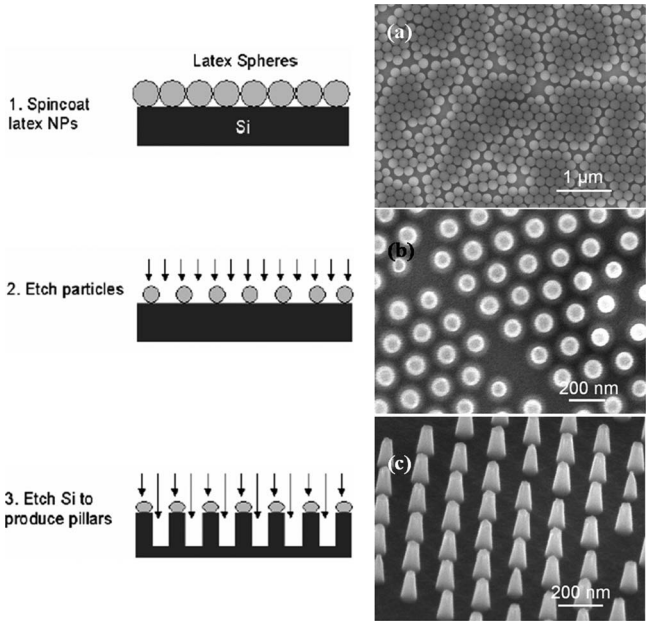

FIG. 4. Process flow showing three steps for nanosphere lithography fabrication of stamps. (a)–(c) are the corresponding SEM images.

ACKOWLEDGMENTS

This work was supported by grants from NIH (Grant No. 1U54CA119367-01), DARPA/Navy (Grant No. N00014-02-1-0807), and Stanford Graduate Fellowship (W.H.). We also acknowledge the use of Stanford Nanofabrication Facility and Stanford Nanocharacterization Laboratory, both partially supported by NSF and Stanford Nanomagnetics facility.

[1] J. H. Lee, Y. M. Huh, Y. Jun, J. Seo, J. Jang, H. T. Song, S. Kim, E. J. Cho, H. G. Yoon, J. S. Suh, and J. Cheon, Nat. Med. **13**, 95 (2007).
[2] C. T. Yavuz, J. T. Mayo, W. W. Yu, A. Prakash, J. C. Falkner, S. Yean, L. L. Cong, H. J. Shipley, A. Kan, M. Tomson, D. Natelson, and V. L. Colvin, Science **314**, 964 (2006).
[3] G. X. Li, S. X. Wang, and S. H. Sun, IEEE Trans. Magn. **40**, 3000 (2004).
[4] R. Hergt, S. Dutz, R. Muller, and M. Zeisberger, J. Phys.: Condens. Matter **18**, S2919 (2006).
[5] S. S. Banerjee and D. H. Chen, Nanotechnology **19**, 265602 (2008).
[6] M. Zeisberger, S. Dutz, R. Muller, R. Hergt, N. Matoussevitch, and H. Bonnemann, J. Magn. Magn. Mater. **311**, 224 (2007).
[7] W. S. Seo, J. H. Lee, X. M. Sun, Y. Suzuki, D. Mann, Z. Liu, M. Terashima, P. C. Yang, M. V. McConnell, D. G. Nishimura, and H. J. Dai, Nature Mater. **5**, 971 (2006).
[8] Y. H. Xu, H. M. Bai, and J. P. Wang, J. Magn. Magn. Mater. **311**, 131 (2007).
[9] W. Hu, C. R. J. Wilson, A. Koh, A. H. Fu, A. Z. Faranesh, C. M. Earhart, S. J. Osterfeld, S. J. Han, L. Xu, S. Guccione, R. Sinclair, and S. X. Wang, Adv. Mater. (Weinheim, Ger.) **20**, 1479 (2008).
[10] B. Dieny and J. P. Gavigan, J. Phys.: Condens. Matter **2**, 187 (1990).
[11] R. J. Wilson, U.S. Patent No. 6,337,215 (8 January 2002).
[12] W. Hu, R. J. Wilson, C. M. Earhart, and S. X. Wang (unpublished).